JOURNAL INDIAN ASSOCIATION OF SEDIMENTOLOGISTS ISSN NO 2582 – 2020
Vol. 38, Issue 1, 2021, pp. 23-32
DOI: https://doi.org/10.51710/jias.v38i1.139

Petro-mineralogical and geochemical characteristics of Shahaba Limestone from Gogi-Kanchankayi sector, Bhima Basin, Karnataka with reference to Uranium mineralisation

Debasish Roy[1], Dheeraj Pande[1], Sikta Patnaik[2], S.K. Varughese[1], A.K. Pradhan[1], B. Saravanan[3], A.K. Bhatt[3]*

Atomic Minerals Directorate for Exploration and Research,
[1]Bengaluru, [2]New Delhi, [3]Hyderabad, *since retired
Corresponding author: debasishroy.amd@gov.in

Abstract

The Shahabad Limestone Formation of Bhima Basin from Gogi-Kanchankayi area occurs in heterogeneous forms like massive/blocky limestone, argillaceous/ siliceous limestone and laminated/ flaggy limestone. These limestones are primarily composed of micrite, which often alters into sparry calcite on diagenesis with associated impurities of quartz, feldspar, barite, chlorite, glauconite, sulphides and carbonaceous matter. Geochemically, these limestones comprises of variable CaO with low MgO and P_2O_5 content. Trace elements concentration shows elevated Ba, Rb and depleted Sr. The current study classified these limestones as non-dolomitic and non-phosphatic types deposited in shallow marine carbonate platform setting with low energy conditions. Post-sedimentation, basin tectonics has resulted in reactivation of the basin margin fault causing intense fracturing of limestone. Subsequent hydrothermal movement along those fractures has resulted in re-mobilisation and re-precipitation of sulphides and carbonaceous matter, and along with alteration has facilitated the precipitation of the uranium bearing minerals.

Keywords: *Gogi-Kanchankayi, Shahabad limestone, Bhima Basin and Uranium Mineralisation*

Introduction

The geochemistry of the carbonate rocks serves as potential tool for evaluating the depositional conditions, degree of diagenesis, tectonic settings, post sedimentation tectonics and provides insights to carbonate deposition (Nagarajan et al., 2011; Sen and Mishra, 2015). Although limestones primarily contain $CaCO_3$, it also comprises of various forms of major and trace elements that are attributed to terrigenous materials and scavenging from seawater (Elderfield and Greaves, 1982). The SiO_2, Al_2O_3, Fe_2O_3, P_2O_5 reflects the mineralogical nature of the carbonates while Mg, Sr, Ba are guiding tools in carbonate facies and diagenesis (Kamber and Webb, 2001; Madhavaraju et al., 2016). Holser (1997) has demonstrated that the elemental type and concentration depends on the plate tectonic environment of the basins. Limestones are liable to post-depositional recrystallization that obliterates primary texture; therefore the relationship between geochemistry of limestones and petromineralogical investigations provide criteria for recognizing ancient plate tectonic environments and secular changes in the chemistry of seawater (Webb and Kamber, 2000). From Gogi-Kanchankayi area the published literature describes the different modes of uranium minerals and pyrite within the deformed Shahabad limestones however; there is a gap in the detailed petrology and geochemistry of the undeformed and non-mineralised limestones of this limestone sequence. The present study focuses on understanding the nature of the Shahabad limestone from Gogi-Kanchankayi traverse (~8 sq. km) and the post sedimentation basin tectonics impact in hosting uranium mineralisation.

Geological Setting

Bhima Basin occurs on the north-western fringe of the Eastern Dharwar Craton and is one of the youngest Meso-Neoproterozoic basins of Peninsular India (Kale and Phansalkar, 1991) (Fig. 1). It is an epicratonic sigmoidal basin where the northern and western extensions are covered by Deccan Trap basaltic flows and, the southern and eastern parts unconformably overlie the basement crystalline rocks comprising of TTG suite of rocks and Closepet Granite and its equivalents (Kale and Peshwa, 1995). Lithostratigraphic succession of the basin by Jayaprakash (1999), shows the Bhima sediments comprising of five formations (Table 1). The Bhima basin exhibits a sequence of an alternation of clastic and carbonate rocks (Akhtar, 1977; Nagarajan et al., 2007). Structurally, the basin is transacted by prominent E-W and NW–SE trending faults besides a number of N-S and NE-SW trending faults. The sediments of the basin are devoid of metamorphism (Kale and Peshwa, 1995).

The Gogi-Kanchankayi is located in the central part of the basin in the vicinity to Kurlagere-Gogi-

Gundanahalli fault (KG fault) (Fig. 2). The KG fault is an east-west trending, ~ 55 km long basin-margin fault that cuts across the sedimentary succession as well as the basement (Chaki et al., 2004). Lithologically, the southern part of the fault exposes basement granitoids while the northern part is occupied by sediments (Achar et al., 1997; Dhana Raju et al., 2002). The area between Gogi-Kanchankayi is largely covered by soil with extensive cultivated lands and limited outcrops. Earlier structural studies on KG fault by the Geological Survey of India (GSI) identified it as a basin margin fault with discernible strike-slip component. Later surface and sub-surface investigations by Atomic Minerals Directorate (AMD) revealed the reverse nature of the fault near Gogi with presence of a cross-fault. Due to reverse faulting, basement granite from the south thrust

Table 1: Stratigraphy of the Bhima Basin

After Jayaprakash (1999)			
Group	Formation	Member	Lithology
Deccan Trap			Basic flows with inter-trappean sediments
Bhima Group	Harwal		Brown, pink to vermillion shale
	Katama devarahalli		Deep grey, occasionally stylolitic flaggy limestone
	Hulkal		Grey, blackish buff, dull and pale pink shale, occasionally with fine grained thin silty beds at the base
	Shahabad	Mulkod Limestone	Deep grey to black flaggy limestone
		Gudur Limestone	Akin to Wadi limestone, yet slightly inferior in chemical composition
		Sedam Limestone	Variegated medium to thickly bedded siliceous limestone
		Wadi Limestone	Thickly bedded, stylolitic, relatively superior cement grade limestone
		Ravoor Limestone	Flaggy limestone with prominent fissility (Shahabad slabs)
	Rabanpalli	Korla shale	Fine silty base, grades into green shale, followed by chocolate brown shale with prominent parting
		Kundrapalle Sandstone	Fine grained quartz arenite, subfelspathic arenite, ferruginous cemented medium grained quartz arenite
		Muddebihal Conglomerate	Pebbly orthoconglomerate, locally or at the top matrix supported and also granular
----------Unconformity ----------			
Basement Crystallines		Younger Granites, Eastern Block Greenstone Belt, Peninsular Gneisses.	

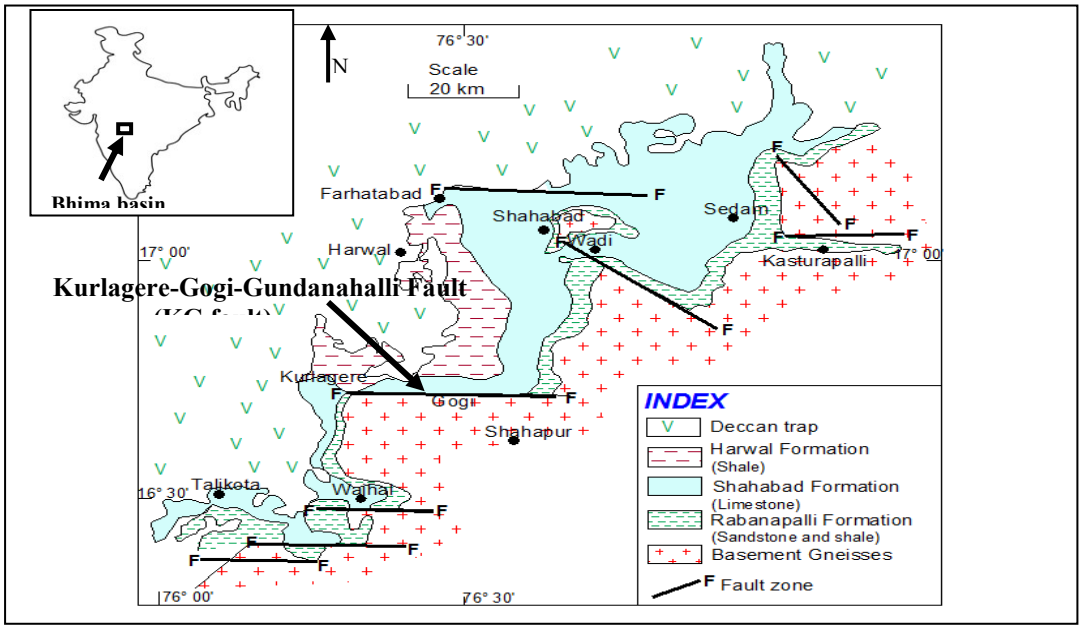

Fig. 1: Regional geological map of Bhima basin showing the location of Kurlagere-Gogi-Gundanahalli fault (modified after Kale and Peshwa, 1995)

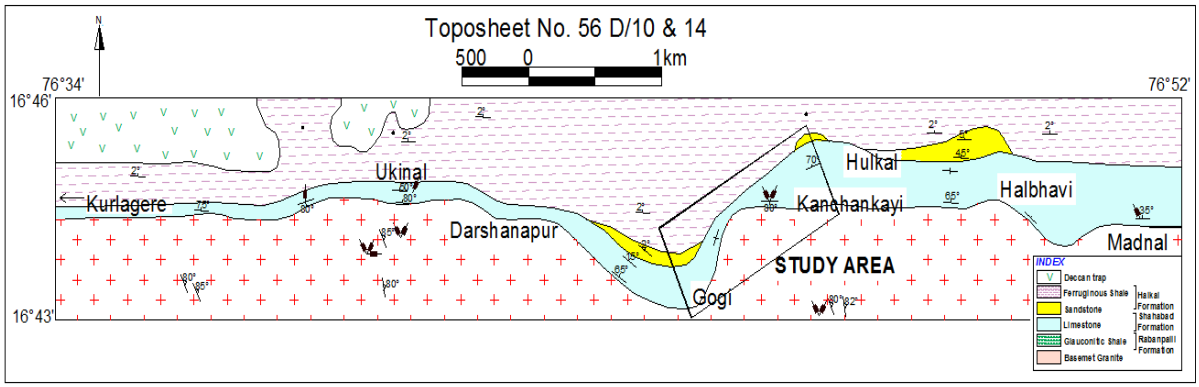

Fig. 2: Geological map around Kurlagere-Gogi-Gundanahalli fault showing the study area (modified after Achar et al., 1997)

over sediments in the north forming a southerly dipping fault (Fig. 3). Recent structural studies by Roy et al. (2016) describe the KG fault as a strike-slip fault with a transpressional zone at Gogi-Kanchankayi sector. In the Gogi-Kanchankayi area the imprints of faulting within the sediments are recorded in the limestones of Shahabad Formation (Fig. 4).

Sampling and Methodology

The study field transact has scanty outcrop and largely covered by soil, hence the research objectives were carried out from sub-surface core samples repository (n=21) of AMD. Petromineralogy study of the polished thin section was carried out in the petrology laboratory of AMD, using a transmitted and reflected light microscope fitted with the image processing unit. Whole rock composition and trace elements were analysed by conventional wet chemical methods at the Chemistry laboratory of AMD. The SiO_2 and P_2O_5 were analysed by UV-visible spectrophotometry (Specord 210); Na_2O, K_2O by flame photometry and LOI by gravimetric methods. FeO is measured by volumetry, TiO_2, Al_2O_3, Fe_2O_3, MnO, CaO, and trace elements were analysed by AAS (Savant AA-GBC scientific Equipment) and ICP-AES (Jy-2000, GBC-Australia).

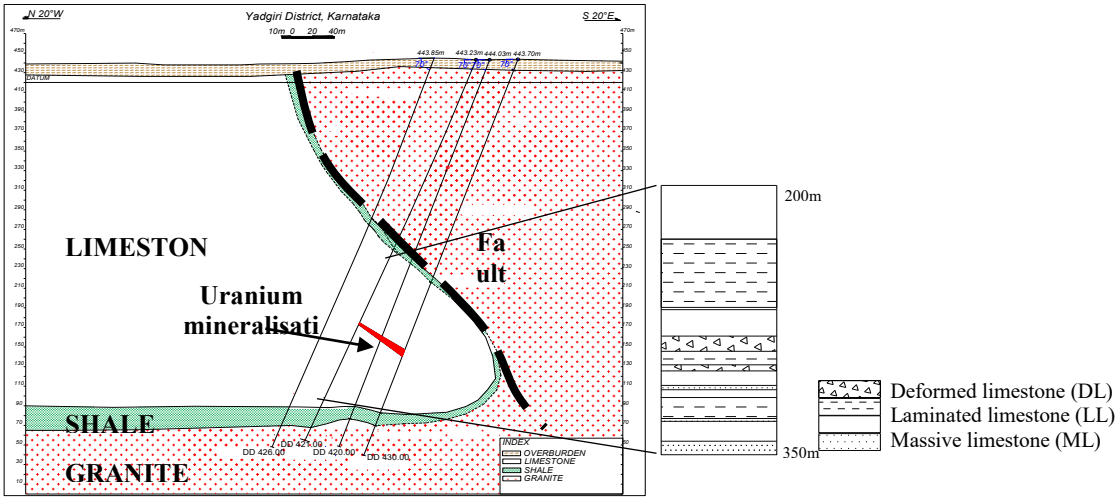

Fig 3: Representative transverse section through boreholes from Kanchankayi area (study area). The dotted line represents trace of the fault plane, inset shows the broad lithology of different types of limestones encountered in the boreholes and red zone shows the uranium mineralisation within the deformed limestones.

Petrography

The sedimentary core section shows three different types of facies of limestone i) laminated/flaggy limestone ii) massive/blocky limestone and iii) argillaceous/siliceous limestone. The post-sedimentation deformation, due to reactivation of the basin margin KG fault has resulted in intense fracturing and brecciation within all the three facies of limestone and it is classified as deformed limestone facies (Fig. 3). The laminated/flaggy limestone (LL) displays alternate light and dark grey laminations, micritic nature with distinct conchoidal fracture (Fig. 5). Silica and calcite veins are parallel to the laminations. The laminations are straight to slightly curvilinear in nature, near parallel to each other with a thickness varying from 0.2-1.0 cm. At places, lenses of clay and packs of quartz grains are forming a load structure causing bending of lamination. Patches of small lumps of pyrite are dispersed throughout the facies. Besides, gypsum, specks of dolomite and barite are noticed. Stylolites are scanty. Microscopically, these samples exhibit cryptocrystalline texture with alternate light and dark lamination (Fig. 6). The recrystallized microspar and sparry calcite are

frequently seen in the facies. The passive filling of the pores and fractures and globular masses of organic matter are noticed at places. The presence of pyrite and carbonaceous matter in the facies suggests existence of the patches of microbial colonies during the deposition of this facies.

Table 2: Major element concentration (wt%) of undeformed Shahabad limestone from Gogi-Kanchankayi area

Sample No	Rock Type	SiO_2	TiO_2	Al_2O_3	Fe_2O_3	FeO	MnO	MgO	CaO	Na_2O	K_2O	P_2O_5	LOI
L-1.	Laminated Limestone (LL)	4.58	0.05	2.11	4.05	0.15	0.02	0.32	52.80	0.12	0.24	0.05	40.47
L-2.		5.33	0.08	2.35	0.70	0.39	0.05	0.57	52.30	1.61	0.63	0.13	35.10
L-3.		7.51	0.04	1.37	0.04	0.24	0.04	0.28	56.55	1.32	0.07	0.13	31.84
L-4.		8.82	0.04	1.47	0.11	0.30	0.03	0.75	46.07	2.66	0.34	0.06	38.69
L-5.		6.48	0.05	2.25	0.22	0.61	0.06	0.85	47.24	2.48	0.72	0.05	38.09
L-6.		5.54	0.04	1.62	0.23	0.49	0.05	0.81	47.50	2.66	0.38	0.08	39.32
L-7		7.58	0.04	1.89	0.40	0.55	0.05	0.75	46.04	1.44	0.45	0.15	39.36
L-8		6.56	0.05	2.10	0.62	0.42	0.03	0.82	47.10	1.36	0.66	0.13	40.12
L-9		8.80	0.04	1.82	0.70	0.61	0.05	0.63	45.90	1.65	0.62	0.09	39.80
	Avg.	6.80	0.05	1.89	0.79	0.42	0.04	0.64	49.06	1.70	0.46	0.10	
M-1.	Massive Limestone (ML)	3.18	0.05	0.67	0.15	0.15	0.03	0.30	53.90	0.20	0.19	0.10	40.90
M-2.		4.69	0.05	1.14	0.05	0.39	0.02	0.50	53.06	0.32	0.33	0.05	40.42
M-3.		4.05	0.05	0.65	0.06	0.24	0.06	4.08	47.39	0.09	0.18	0.10	41.88
M-4.		4.89	0.04	1.57	0.28	0.30	0.05	0.49	51.20	1.06	0.23	0.06	39.62
M-5.		4.80	1.64	1.24	0.12	0.61	0.05	0.39	49.29	1.05	0.23	0.08	39.58
M-6.		3.20	0.02	0.72	0.11	0.49	0.03	3.11	53.65	0.32	0.22	0.05	38.09
M-7		4.12	0.07	1.12	0.15	0.55	0.03	1.8	53.60	1.02	0.3	0.08	37.1
M-8		3.85	0.05	0.76	0.2	0.2	0.03	2.62	51.85	0.09	0.2	0.06	39.65
	Avg.	4.10	0.25	0.98	0.13	0.35	0.04	1.66	51.74	0.52	0.23	0.07	
S-1	Siliceous limestone (SL)	30.05	0.06	1.27	0.09	0.30	0.03	0.23	38.80	0.18	0.36	0.30	29.25
S-2		32.51	0.05	1.18	0.10	0.38	0.07	0.37	36.90	0.12	0.29	0.19	28.24
S-3		29.05	0.06	1.37	0.09	0.30	0.06	0.35	36.80	0.18	0.36	0.30	30.25
S-4		30.51	0.05	1.21	0.11	0.30	0.07	0.27	37.90	0.13	0.29	0.20	28.24
S-5		31.25	0.05	1.36	0.08	0.30	0.07	0.31	38.90	0.13	0.29	0.20	26.24
S-6		30.85	0.06	1.25	0.09	0.36	0.06	0.23	37.80	0.14	0.36	0.30	29.25
	Avg.	30.70	0.05	1.27	0.09	0.32	0.06	0.29	37.85	0.15	0.33	0.25	
D-1.	Deformed /Mineralised Limestone (DL)	19.88	0.61	2.87	2.73	2.94	0.02	1.36	42.34	1.17	2.41	0.31	22.97
D-2.		17.41	0.51	4.84	3.26	2.11	0.02	0.57	42.66	0.92	1.56	0.15	23.08
D-3.		15.09	0.03	1.37	0.74	0.43	0.13	0.32	45.16	1.100	0.15	0.040	35.26
D-4.		16.65	0.11	3.47	14.65	2.16	0.29	0.53	33.01	0.940	0.46	0.170	25.93
D-5.		26.72	0.38	8.66	15.83	4.25	0.20	1.08	21.99	0.730	0.84	0.260	17.92
	Avg.	19.15	0.31	4.24	7.44	2.38	0.13	0.77	37.03	0.97	1.08	0.19	

The massive/blocky limestone (ML) is devoid of laminations and displaying light grey to yellowish grey colour (Fig. 7). Stylolites are distinct which are parallel, inclined and vertical with respect to the bedding plane (Fig. 8). Based on the geometry, the stylolites were classified as wavy and suture type which at places are filled with secondary calcite and pyrite. Secondary silica and twinned calcite veins are present. Minor deformation evidences like micro-faults, intraformational brecciation and shear bands are recorded at places.

The siliceous limestone (SL) is similar to ML but it varies in presence of grains of detrital quartz with less feldspars which is arranged in the form of layers resting over the micritic mass. In the core samples, silica banding is not visible but under microscope it shows parallel lamination (Figs. 9 and 10). This observation indicates the increase in the influx of the detrital material during its precipitation. The SL facies occurs intermediate between LL and ML facies indicating episodic supply of siliciclastic materials.

Fig 4: Steeply dipping limestones reflect surface expression of the Kurlagere-Gogi-Gundanahalli fault. Location: West of Gogi.

Deformed limestone (DL) is the result of post depositional deformation (faulting). This facies is moderate to highly brecciated, altered and having angular clasts of limestone of different sizes cemented by secondary calcite and chloritic cement (Fig. 11). Mineralogically, it is composed of micritic and sparry calcite along with varying amounts of quartz, chalcedony, chert, feldspar, barite, chlorite, clay, limonite, illite and sulphides. It is rich in sulphide veins, predominantly pyrite along with cross cutting calcite and silica veins (Fig. 12). Few core samples are dark grey in colour containing carbonaceous matter and clasts of basement granite and shale. Faulting and subsequent fault related fluid movement has resulted in its extensive hydrothermal alteration.

Geochemistry

Major Elements

Major element concentrations of the LL, ML, SL and DL are presented in Table 2. It is observed that the CaO in the LL and ML varies from 45.90% to 56.55% (avg. 49.06%, n = 9) and to 47.39% to 53.90% (avg. 51.74%, n = 8) respectively. Six samples analysed from (SL) horizon show lower CaO as compared to LL and ML i.e. 36.80% to 38.90% (avg. 37.85%, n = 6). SiO_2 content in LL and ML is 4.58% to 8.82% (avg. 6.80%) and 3.18% to 4.89% (avg. 4.10%) respectively, while in SL it is 29.05% to 32.51% (avg. 30.70%) indicating significant clastic input compared to LL and ML. SiO_2 vs CaO in LL and ML depicts a negative correlation, suggesting a relatively lower carbonate precipitation rate during clastic influx (Fig. 15a). The P_2O_5 and MgO content of LL, ML and SL vary from 0.05% to 0.30% and 0.30% to 4.08% respectively, indicating a low Mg and low P type. Al_2O_3 shows wide variations from 0.65% to 2.35%. A positive correlation exists between SiO_2 vs P_2O_5 in LL while SL is more phosphatic than the other two types of limestones (Fig. 15b). A scattered relationship between Sr and Al_2O_3 in all three types of limestones indicates the absence or insignificant proportion of the plagioclase as one of the phases (Fig. 15c). A relatively higher concentration of Fe_2O_3 in one sample (L-1) is probably the reflection of the clay minerals associated with it. MnO in all of the samples varies within a range of 0.02% to 0.07%. The low MnO content is subtle to the fact that it was deposited in the shallow marine environment in low energy conditions. The LL, ML and SL samples recorded low content of TiO_2, Na_2O and K_2O.

In DL it is observed that the CaO varies from 21.99% to 45.16% (avg. 37.03%) which is lower than that of the undeformed limestone indicating removal of carbonate minerals. In DL, there is an increase in SiO_2 content ranging from 15.09% to 26.72 (avg. 19.15%) as compared to LL and ML. The high SiO_2 content of SL is due to the presence of silica as detritus while elevated SiO_2 content of DL corresponds to the presence of silica veins formed during deformation and subsequent hydrothermal alterations. The P_2O_5 and MgO content of DL remains the same as in LL, ML and SL (Fig. 15d). The variation of CaO and SiO_2 between the deformed and undeformed limestones is shown in the binary plot (Fig. 15e). This also shows a negative correlation in deformed limestone. There is an increase of Al_2O_3 and Fe_2O_3 in DL possibly due to clay formation in the deformed and mineralised zone. K_2O/Al_2O_3 vs MgO/Al_2O_3 infers the clay is mostly illite (Fig. 15f).

Trace elements

Trace element concentration of LL, ML and SL (n = 23) displays the low concentration of Cu, Co, Ni, Zn, Mo with an enriched concentration of Sr, Rb and Ba (Table 3). The ML showed up to 1888ppm of Ba and Sr up to 202 ppm which is lower than the average Proterozoic carbonates (Sr = 610 ppm, Turekian and Wadepohl, 1961). The Ba content is higher as compared

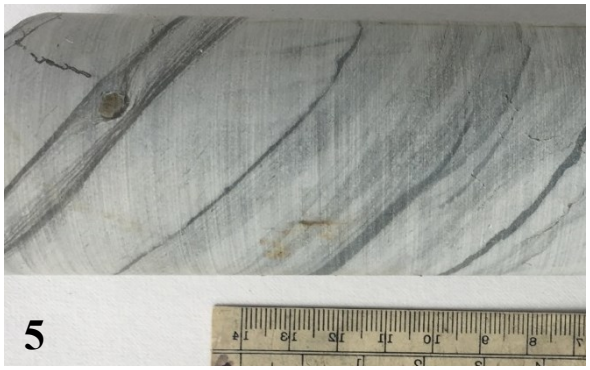

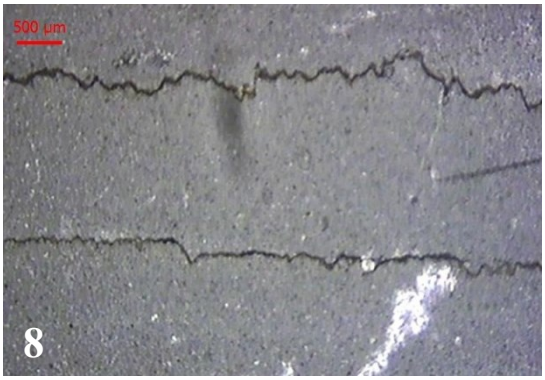

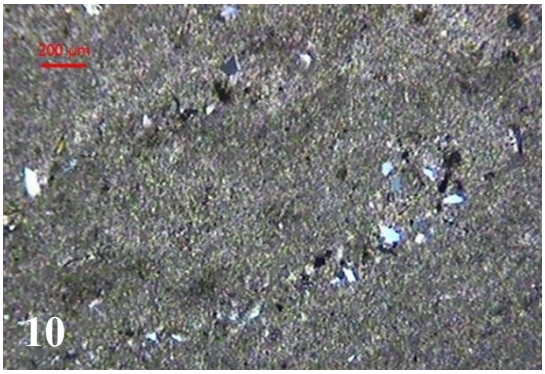

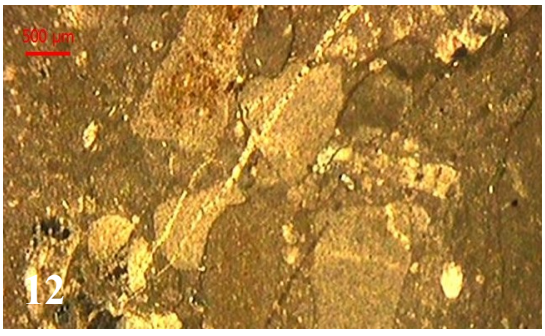

Fig. 5: Core of laminated limestone showing alternate dark and light colour laminations and a small lump of pyrite; location: Kanchankayi; Core size: NQ (Dia-47.6mm) Fig. 6: Photomicrograph of laminated limestone showing the persistent parallel lamination and clay lenses, 5X, TL, 1N. Fig. 7: Massive limestone with stylolites; Location: Kanchankayi; Core size: NQ (Dia-47.6mm) Fig. 8: Massive limestone with parallel stylolites, 5X, TL, 1N. Fig. 9: Siliceous limestone; Location: Kanchankayi; Core size: NQ (Dia-47.6mm) Fig. 10: Siliceous limestone with detrital fragments of quartz parallel to laminations; 5X, TL, 1N. Fig. 11: Deformed limestone showing brecciation and alterations; Location: Kanchankayi; Core size: NQ (Dia-47.6mm). Fig. 12: Brecciated limestone with brecciated fragments of micrite and sparry calcite are set in micritic limestone. 5X, TL, 1N.

Fig. 13: Core of brecciated pyritiferous uranium mineralised limestone; location: Kanchankayi; Core:NQ (Dia-47.6mm)
.

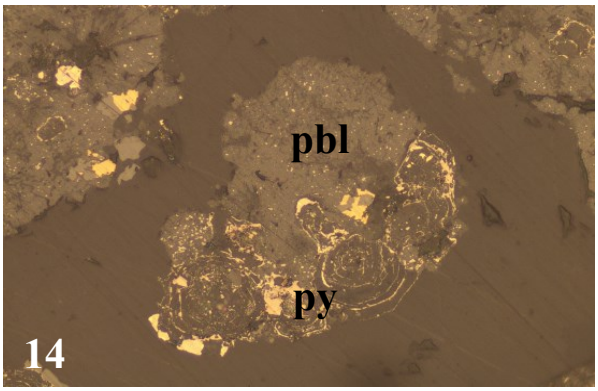

Fig. 14: Photomicrograph of mineralised limestone showing pitchblende (pbl) and pyrite (py) association, 20X, RL, XN

to the marine carbonate i.e. <60 ppm (Friedman, 1969). The abundance of Mn and Sr has been recognised as an interpretive tool to evaluate the diagenetic history of the carbonate (Viezer, 1983). Mn may be incorporated and Sr may be expelled from the carbonate system during diagenesis (Viezer, 1983). Mn/Sr ratio of 1-3 is accepted as an indicator of diagenetically unaltered limestone (Viezer, 1983; Jacobsen and Kaufman, 1999). The Mn/Sr ratio for the LL and ML is < 3 indicating these limestones were not subjected to severe diagenetic alteration. Mn/Sr ratio for SL is >3 and this may be due to the presence of higher amount SiO_2. Trace element concentration of the DL (n = 5) shows contrast with respect to undeformed limestone (Table 4). It comprises of elevated concentration of Cu (18 - 490ppm), Co (65-770ppm), Ni (12 - 85ppm), Zn (10-165ppm), Mo (15-85ppm) and Cr (20 - 195ppm). The high concentration of the trace elements within the deformed limestone is attributed to the post sedimentation tectonics and followed by hydrothermal alterations.

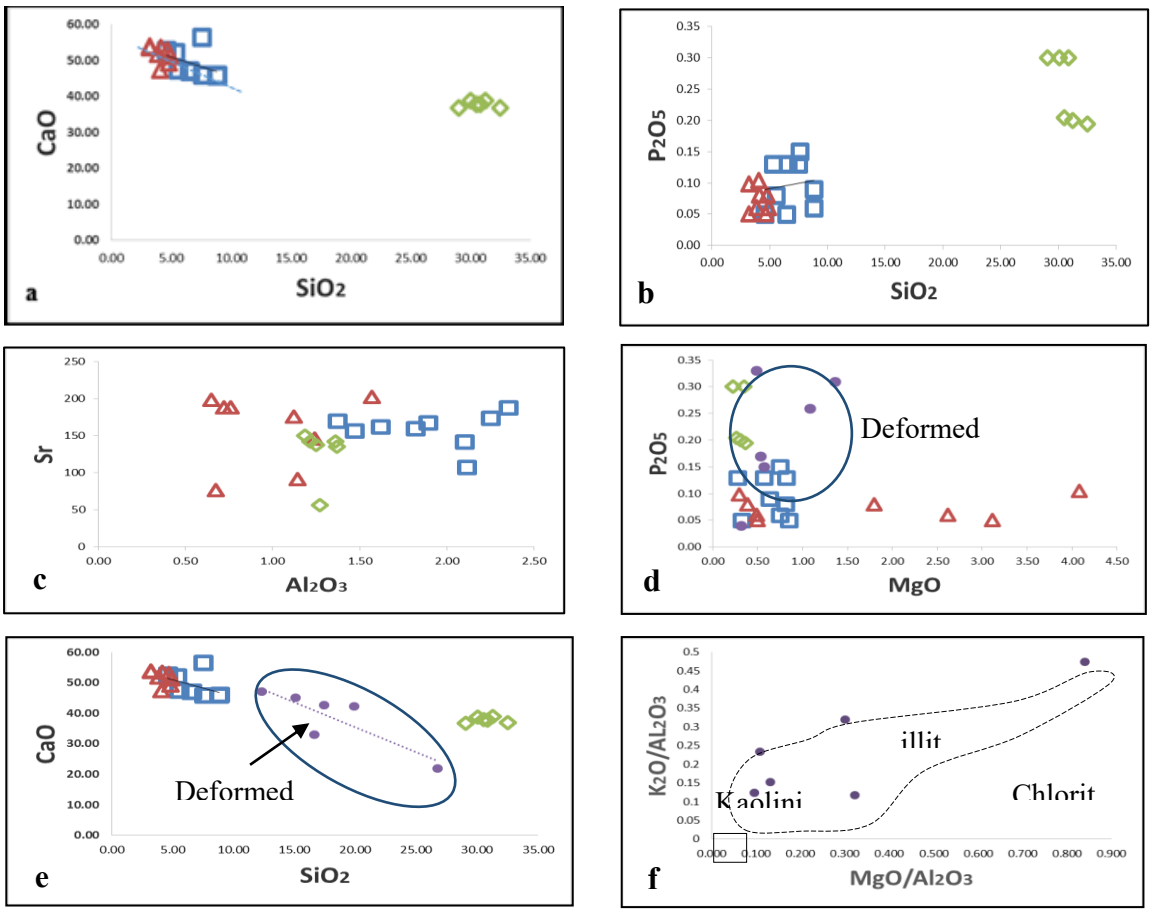

Fig 15 (a-f): Bivariate plots for the Shahabad limestones.

Laminated limestone Massive limestone Siliceous Deformed limestone

Uranium mineralisation

In Gogi-Kanchankayi sector, uranium mineralisation is associated with deformed limestone (DL). The deformation is due to the post-sedimentation tectonic movement along the KG fault which has resulted in the development of fracture and breccia zones, induced secondary porosity in the LL, ML and SL facies of Shahabad Limestone thus aiding in the generation and migration of the uranium rich hydrothermal fluids. The younger granitoids of Closepet equivalent, within the basement, are the likely source for uranium rich hydrothermal fluids. Pitchblende and coffinite uranium minerals were identified (Fig. 13). The fracture/breccia zones within LL, ML and SL are rich in sulphides and carbonaceous matter that host the uranium mineralisation. Pyrite is the major constituent of sulphides and occurs in different morphological and textural varieties viz., lumpy, reticulate, botryoidal, oolitic, porous and zoned. Besides, other ore minerals identified are galena, chalcopyrite, pyrolusite, arsenopyrite, nicolite and cobaltite. The mineralised zones are invariably associated with sulphides and carbonaceous matter (Fig. 14). Patnaik et al. (2016) reported that the TOC content for mineralised deformed limestone varies from 34.3- 51.1 wt% (avg. 42.27wt %, n = 4). The undeformed Shahabad limestone is the probable source for the carbonaceous matter and sulphi-

Table 3: Trace element concentration (ppm) of undeformed Shahabad limestone from Gogi-Kanchankayi area

Sample No	Rock Type	Cu	Co	Ni	Rb	Zn	Pb	V	Sr	Zr	Mo	Ba	Ga	Mn	Mn/Sr
L-1.	Laminated Limestone (LL)	<10	<10	<10	11	<10	<25	<10	107	10	<10	56	<10	158	1.47
L-2.		12	<10	<10	11	<10	30	<10	188	<10	<10	60	<10	387	2.06
L-3.		<10	<10	<10	11	10	30	<10	170	<10	<10	82	<10	310	1.82
L-4.		10	<10	<10	9	<10	<25	<10	157	15	<10	145	<10	232	1.48
L-5.		<10	<10	<10	32	<10	<25	23	174	12	<10	80	<10	465	2.67
L-6.		<10	<10	<10	12	12	<25	<10	162	10	<10	175	<10	387	2.39
L-7		<10	<10	<10	20	12	<25	<10	168	10	<10	150	<10	387	2.36
L-8		<10	<10	<10	12	<10	30	<10	142	<10	<10	96	<10	232	1.62
L-9		<10	<10	<10	18	10	<25	<10	160	12	<10	142	<10	387	2.42
M-1.	Massive Limestone (ML)	<10	<10	<10	10	10	<25	<10	77	10	<10	52	<10	226	2.94
M-2.		<10	<10	<10	18	10	<25	<10	92	10	<10	46	<10	168	1.82
M-3.		10	<10	<10	10	<10	<25	10	198	<10	<10	1888	<10	503	2.53
M-4.		10	<10	<10	10	<10	<25	10	202	<10	<10	560	<10	387	1.91
M-5.		14	<10	<10	15	<10	30	<10	116	<10	<10	48	<10	387	2.65
M-6.		<10	<10	<10	18	10	<25	<10	188	10	<10	72	<10	232	1.23
M-7		<10	<10	<10	12	12	<25	<10	176	10	<10	72	<10	232	1.32
M-8		10	<10	<10	10	10	<25	<10	188	<10	<10	250	<10	232	1.24
S-1	Siliceous limestone (SL)	<10	<10	<10	16	15	<25	<10	57	16	<10	107	<10	223	3.95
S-2		<10	<10	<10	10	10	<25	<10	150	11	<10	98	<10	536	3.56
S-3		<10	<10	<10	12	<10	<25	<10	135	11	<10	120	<10	456	3.37
S-4		<10	<10	<10	11	12	<25	10	142	12	<10	110	<10	536	3.77
S-5		<10	<10	<10	11	12	<25	10	142	12	<10	110	<10	542	3.81
S-6		<10	<10	<10	12	11	<25	10	138	12	<10	105	<10	464	3.36

Table 4: Trace element concentration (ppm) of deformed Shahabad limestone from Gogi-Kanchankayi area

Sample No	Rock Type	Cu	Co	Cr	Ni	Zn	Pb	V	Zr	Mo
D-1.	Deformed /Mineralised Limestone (DL)	490	65	195	25	165	1770	693	55	85
D-2.		155	770	175	65	150	7825	1545	50	25
D-3.		18	85	20	12	25	259	118	30	15
D-4.		75	152	65	30	10	375	50	60	15
D-5.		100	350	60	85	120	290	525	60	50

des which are re-mobilised and re-precipitated during deformation and act as a reductant for precipitation of uranium from the hydrothermal fluid within the fractures. The prominent hydrothermal alteration along the mineralised zone are chloritisation, silicification, calcification, hematitisation, illitisation and kaolinisation, which are distinct from the non-mineralised limestones. Hydrothermal alteration has resulted in depletion of CaO, with an increase in SiO_2, Al_2O_3, Fe_2O_3, Cu, Co, Ni, Zn, Mo and Cr. The depletion of CaO is an indication of the dissolution of limestone by hydrothermal fluid developing secondary porosity. The sulphides and carbonaceous matter along with alterations in the fracture zones have controlled the reduction of uranium from the hydrothermal fluids.

Conclusions

The study of sub-surface limestone core samples from Gogi-Kanchankayi sector revealed three different types of facies viz. massive/blocky, argillaceous/siliceous and laminated/flaggy limestones.
The results of this study suggest that these limestones are micritic, non-dolomitic and non-phosphatic in nature with quartz (as detrital grains), sulphides (pyrite) and patches of carbonaceous matter as impurities.
These limestone facies were deposited under shallow marine setting in low energy conditions with Mn/Sr ratio range of 1.4 to 3.5 indicating that these rocks are partially diagenetically altered.

Post sedimentation deformation associated with faulting resulted in the development of fractures and breccia zones, inducing secondary porosity and thus aiding the migration of hydrothermal fluids. Precipitation and deposition of remobilised sulphides and carbonaceous matter along with alteration in the fracture / breccia zones during pre-ore and syn-ore stages facilitated adsorption and reduction of uranium from the hydrothermal fluids.

Acknowledgement

The authors are thankful to the Director AMD, for granting permission to publish this work. Constructive suggestions and comments by anonymous reviewers which helped in improving the quality of the manuscript are thankfully acknowledged. Colleagues in the Chemistry laboratory, AMD, Bengaluru are gratefully acknowledged for providing the analytical facilities.

References

Achar, K.K., Pandit, S.A., Natarajan, V., Kumar, M. K. and Dwivedy, K.K. (1997). Uranium mineralisation in the Neoproterozoic Bhima Basin, Karnataka, India. In: Recent Developments in Uranium Resources, Production and Demand, *IAEA,* Vienna, 1-22.

Akhtar, K. (1977). Depositional environment, dispersal pattern and palaeogeography of the clastic sequence in the Bhima Basin. *Indian Mineralogist*, 18, 65–72.

Chaki, A., Pandit, S.A. and Achar, K.K. (2004). An appraisal of uranium exploration in the Kaladgi-Badami and Bhima basins in Karnataka and identification of potential targets for uranium exploration by Geophysical Methods. *Exploration and Research for Atomic Minerals*, 15, 13-24.

Dhana Raju, R., Kumar, M.K., Babu, E.V.S.S.K. and Pandit, S.A. (2002). Uranium mineralisation in the Neo-Proterozoic Bhima Basin at Gogi and near Ukinal – Ore petrology and mineral chemistry. *Journal of the Geological Society of India*, 59, 299-321.

Elderfield, H. and Greaves, M.J. (1982). The rare earth elements in seawater. *Nature,* 296, 214–219.

Friedman, G.M. (1969). Trace elements as possible environmental indicators in carbonate sediments. In Friedman G.M. (Ed.), Dolomitisation and limestone diagenesis. *Society Eon. Paleon. Mineral Special Publication,* 13, 14-48.

Holser, W.T. (1997). Evaluation of the application of rare earth elements to paleoceanography. *Palaeogeography, Palaeoclimatology, Palaeoecology,* 132, 309-323.

Jacobsen, S.B. and Kaufman, A.J. (1999). The Sr, C and O isotopic evolution of Neoproterozoic seawater. *Chemical Geology,* 161, 37–57.

Jayaprakash A.V. (1999). Evolutionary history of Bhima basin. (V.S. Kale and R.H. Sawkar, Compilers), *Journal of the Geological Society of India,* 23–28.

Kamber, B.S. and Webb, G.E. (2001). The geochemistry of late Archaean microbial carbonate: Implications for ocean chemistry and continental erosion history. *Geochimica et Cosmochimica Acta,* 65, 2509-2525.

Kale, V.S. and Phansalkar, V. G. (1991). Purana basin of Peninsular India: a review. *Basin Research,* 3, 1-36.

Kale, V.S. and Peshwa, V.V. (1995). Bhima Basin. *Geologial Society of India publication,* Bangalore, 10.

Madhavaraju, J., Löser, H., Lee, Y.I., Santacruz, R.L. and Pi-Puig, T. (2016). Geochemistry of Lower Cretaceous limestones of the Alisitos Formation, Baja California, Mexico: Implications for REE source and paleo-redox conditions. *Journal of South American Earth Sciences,* 66, 149–165.

Nagarajan, R., Madhavaraju, J., Nagendra, R., Altrin, J.S.A. and Moutte, J. (2007). Geochemistry of Neoproterozoic shales of the Rabanpalli Formation, Bhima Basin, Northern Karnataka, southern India: implications for provenance and paleoredox conditions. *Revista Mexicana de Ciencias Geológicas,* 24, 150–160.

Nagarajan, R., Madhavaraju, J., Armstrong-Altrin, J.S. and Nagendra, R. (2011). Geochemistry of neoproterozoic limestones of the Shahabad formation, Bhima basin, Karnataka, southern India. *Geosciences Journal,* 15, 9–25.

Patnaik, S., Chakrabarti, K., Pradhan, A. K. and Bhattacharya, D. (2016). Petrographic characteristics of carbonaceous matter associated with brecciated limestone at Kanchankayi area, Yadgir district, Karnataka: Genetic implications for uranium mineralization. *Journal of Applied Geochemistry*, 18 (3), 119-124.

Roy, D., Bhattacharya, D., Mohanty, R., Patnaik, S., Pradhan, A.K., Chakrabarti, K. and Syed Z. (2016). Study of Deformation pattern in Gogi-Kurlagere fault zone at Gogi-Kanchankayi sector of Proterozoic Bhima Basin of northern Karnataka: its implication in control of uranium mineralisation. *Journal of Exploration and Research for Atomic Minerals,* 26, 157-176.

Sen, S. and Mishra, M. (2015). Geochemistry of Rohtas limestone from Vindhyan Supergroup, Central India: evidences of detrital input from felsic source. *Geochemistry International,* 53, 1107–1122.

Turekian K. K. and Wedepohl, H. K. (1961). Distributions of the elements in some major units of earth crust. *Geological society of America bulletin,* 72, 175-192.

Veizer, J. (1983). Trace elements and isotopes in sedimentary carbonates, in Reeder, R.J. (ed.), Carbonates: Mineralogy and Chemistry. *U.S.A, Mineralogical Society of America, Reviews of Mineralogy*, 11, 265-299.

Webb, G.E. and Kamber, B.S. (2000). Rare earth elements in Holocene reefal microbialites: a new shallow seawater proxy. *Geochimica et Cosmochimica Acta,* 64, 1557–1565.

(Received: 17 September 2020; Revised version accepted: 30 May 2021)